JOURNAL OF COMPUTATIONAL PHYSICS **83**, 324–344 (1989)

A Comparison of Fourier Pseudospectral Methods for the Solution of the Korteweg–de Vries Equation

F. Z. NOURI AND D. M. SLOAN

Department of Mathematics, University of Strathclyde,
Glasgow G1 1XH, Scotland

Received April 15, 1988; revised August 11, 1988

Various Fourier pseudospectral methods are used to approximate the Korteweg–de Vries equation. The methods differ in their treatment of the time discretisation. The methods are compared for computational efficiency using the 1- and 2-soliton test problems. They are also compared from an accuracy viewpoint using the Zabusky–Kruskal recurrence problem.

1. INTRODUCTION

The interest in nonlinear wave phenomena has experienced a rapid growth in recent years and the Korteweg–de Vries equation (KdV) has played a central role in this recent development. The KdV equation was originally introduced [8] to describe the behaviour of small amplitude water waves in one dimension. More recently the equation has been used to describe phenomena such as ion-acoustic waves in plasma physics, longitudinal dispersive waves in elastic rods, and pressure waves in liquid-gas bubble mixtures. Nonlinear dispersive wave equations, as typified by the KdV equation, exhibit an array of fascinating solutions such as solitary waves, solitons, and recurrence [3]. The existence of such solutions, together with the ubiquity of specific equations like the KdV, has been the source of the intense interest in this type of partial differential equation.

The inverse scattering method has been used to produce some analytic solutions of nonlinear dispersive wave equations such as the KdV equation [6]. However, its usefulness as a general tool is limited, and the availability of accurate and efficient numerical methods is therefore essential. The numerical solution of nonlinear dispersive wave equations has been the subject of many papers over the last two decades. Zabusky and Kruskal [20] employed a second-order accurate leap-frog scheme for the KdV equation. Dissipative difference methods were used by Vliegenthart [19], Galerkin methods by Alexander and Morris [1], and Petrov–Galerkin methods by Sanz-Serna and Christie [11] and by Schoombie [15].

Ideally a numerical method should be free of phase errors and it should simulate the conservation properties of the differential equation. These properties have been

0021-9991/89 $3.00

discussed by Sanz-Serna [12] and he has proposed a variable-step method which satisfies the first two of the infinite set of conservation conditions associated with the KdV equation. Taha and Ablowitz [17] used the inverse scattering transform to construct a global scheme which satisfies the complete set of conservation laws. However, this interesting scheme is likely to be too complicated to be of much practical use. A second scheme is proposed by Taha and Ablowitz [17] which, albeit fully, implicit, is much less cumbersome. This so-called local scheme seems to be very attractive in terms of computational efficiency, as pointed out in the following paragraph.

Fourier spectral methods have been applied to the KdV equation by, for example, Tappert [18], Schamel and Elsässer [14], Fornberg and Whitham [5], and Chan and Kerkhoven [2]. A recent study by Taha and Ablowitz [17] compared the efficiencies of various numerical methods for the KdV equation. Their study included the Fourier pseudospectral method of Fornberg and Whitham [5], together with an improved form of the split-step Fourier method proposed by Tappert [18]. Results obtained by Taha and Ablowitz suggest that the Fourier spectral method provides an extremely efficient numerical method for the KdV equation. In the efficiency tests the authors found that the best method was their aforementioned local scheme and that this was followed closely by the pseudospectral method of Fornberg and Whitham [5]. These findings provide some motivation for the present study. The aim here is to extend the valuable study of Taha and Ablowitz to compare several Fourier pseudospectral methods. We are particularly interested in comparing methods which adopt different approaches to the time discretisation. Our search for an efficient time-stepping technique will initially follow the same lines as those adopted by Taha and Ablowitz. We use various methods to integrate the equation

$$u_t + 6uu_x + u_{xxx} = 0 \tag{1.1}$$

over a time interval from $t=0$ to $t=T$, with initial conditions which match the analytic 1-soliton and 2-soliton solutions (see, for example, Hirota [7]). Details of these test problems, together with comments on the spatial discretisation of (1.1), are given in Section 2. For the efficiency comparison the maximum acceptable point-wise error at $t=T$ is specified and the parameters such as time-step are adjusted to minimise the computing time, subject to this error constraint. Section 3 describes the various time-stepping methods used in the efficiency tests and Section 4 gives numerical results for these tests.

In Section 4 the pseudospectral methods are also compared from an accuracy viewpoint by investigating how capable they are of reproducing the recurrence phenomenon described by Zabusky and Kruskal [20]. Comments and conclusions are contained in Section 5.

2. One- and Two-Soliton Test Problems

The exact 1-soliton solution of (1.1) on the infinite interval is

$$u(x, t)=2k^2 \operatorname{sech}^2(kx-4k^3t+\eta_0), \tag{2.1}$$

where k and η_0 are constants, with $k>0$. This represents a soliton of amplitude $2k^2$ initially located at $x=-\eta_0/k$ and moving with velocity $4k^2$.

The exact 2-soliton solution of (1.1) on the infinite interval is

$$u(x, t)=2\frac{\partial^2}{\partial x^2}[\log_e f(x, t)], \tag{2.2}$$

with

$$f(x, t)=1+e^{\eta_1}+e^{\eta_2}+\left(\frac{k_1-k_2}{k_1+k_2}\right)^2 e^{(\eta_1+\eta_2)}$$

and

$$\eta_i=\eta_i(x, t)=k_i x-k_i^3 t+\eta_i^{(0)},$$

where k_i and $\eta_i^{(0)}$ are constants for $i=1, 2$. The constants k_1 and k_2 are both taken to be positive. For $i=1, 2$ soliton i has amplitude $k_i^2/2$ and it is moving with velocity k_i^2 from an initial location $x=-\eta_i^{(0)}/k_i$.

To permit a numerical solution of (1.1) we assume that the 1- and 2-soliton solutions satisfy the periodicity condition $u(x+2L, t)=u(x, t)$, for $(x, t)\in \mathbb{R}\times[0, T]$. Accordingly, we consider numerical solutions in the region $-L\leqslant x\leqslant L$, with the positive constant L sufficiently large for the periodicity condition to be acceptable. To simplify the presentation of Fourier methods it is now convenient to transform the spatial variable in (1.1) to $X=(\pi/L)(x+L)$, giving a 2π-periodic dependent variable $v(X, t)$ which satisfies

$$v_t+6svv_X+s^3v_{XXX}=0, \qquad (X, t)\in\mathbb{R}\times[0, T], \tag{2.3}$$

with s denoting π/L.

To solve (2.3) by a pseudospectral method the interval $[0, 2\pi]$ is discretised by $N+1$ equidistant points with spacing $\Delta X=2\pi/N$, and $v(\cdot, t)$ is approximated by $V(\cdot, t)\in\mathbb{R}^N$, which has the value $V(X_j, t)$ at $X=X_j=j\Delta X$, $j=0, 1, ..., N-1$. The vector $V(\cdot, t)$ is transformed to discrete Fourier space by

$$\begin{aligned}\hat{V}(p, t)=(FV(\cdot, t))(p)=\frac{1}{\sqrt{N}}\sum_{j=0}^{N-1} V(X_j, t)\, e^{-2\pi ijp/N},\\ p=-\frac{N}{2}, -\frac{N}{2}+1, ..., \frac{N}{2}.\end{aligned} \tag{2.4}$$

We assume N is even, with $M=N/2$, and note that $\hat{V}(-M,t)=\hat{V}(M,t)$. One should also note, of course, that since $V(\cdot,t)\in\mathbb{R}^N$ then $\hat{V}(0,t)$ and $\hat{V}(M,t)$ are real and $\hat{V}(-p,t)$ is the complex conjugate of $\hat{V}(p,t)$ for $p=1,2,\dots,M-1$. The inversion formula for the discrete Fourier transform (2.4) is

$$V(X_j,t)=(F^{-1}\hat{V}(\cdot,t))(X_j)=\frac{1}{\sqrt{N}}\sum_{p=-M}^{M-1}\hat{V}(p,t)\,e^{2\pi ijp/N},\qquad j=0,1,\dots,N-1. \tag{2.5}$$

The transformations in (2.4) and (2.5) can be performed efficiently by means of the fast Fourier transform algorithm (FFT). Derivatives of v with respect to X may also be approximated efficiently by the FFT algorithm: for example, the qth derivative at (X_j,t) is given by $(F^{-1}\hat{Z}(\cdot,t))(X_j)$, where $\hat{Z}(p,t)=(ip)^q\,\hat{V}(p,t)$. Fornberg [4] has shown how this representation of derivatives of periodic functions is related to central difference approximations of infinite order.

Periodic solutions of (2.3) satisfy an infinite sequence of conservation laws and the accuracy of the numerical solutions of the test problems is checked using two of these laws. Like Taha and Ablowitz, we approximate the conditions

$$\int_0^{2\pi}[v(X,t)]^2\,dX=C_1 \tag{2.6}$$

and

$$\int_0^{2\pi}\{2[v(X,t)]^3-s^2[v_X(X,t)]^2\}\,dX=C_2 \tag{2.7}$$

using Simpson's rule and compare these approximations to the exact values of C_1 and C_2.

3. Numerical Methods Used for the KdV Equation

The following pseudospectral schemes are used to approximate the 1- and 2-soliton solutions of (1.1):

(i) the leap-frog scheme of Fornberg and Whitham [5];
(ii) the semi-implicit scheme of Chan and Kerkhoven [2];
(iii) the modified basis function scheme of Chan and Kerkhoven [2];
(iv) a split-step scheme based on Taylor expansion;
(v) a split-step scheme based on characteristics;
(vi) a quasi-Newton implicit method.

Method (i) was considered by Taha and Ablowitz [17] and it is included in order to provide a link between their comparative study and the present work. This was the more efficient of the two Fourier methods considered by Taha and Ablowitz.

3.1. *Outline of methods* (i), (ii), *and* (iii)

(i) *Fornberg and Whitham* [5]. If we approximate spatial derivatives in (2.3) using discrete Fourier transforms, as described in Section 2, and combine this with a leap-frog discretisation in time we obtain

$$\begin{aligned} V(X_j, t+\Delta t) = V(X_j, t-\Delta t) - 12s\,\Delta t\, V(X_j, t)(F^{-1}(ip\hat{V}(p, t)))(X_j) \\ + 2s^3\,\Delta t(F^{-1}(ip^3\hat{V}(p, t)))(X_j), \end{aligned} \tag{3.1}$$

where Δt denotes the time step. Fornberg and Whitham modified the final term in (3.1) to produce the scheme

$$\begin{aligned} V(X_j, t+\Delta t) = V(X_j, t-\Delta t) - 12s\,\Delta t i V(X_j, t)(F^{-1}(p\hat{V}(p, t)))(X_j) \\ + 2i(F^{-1}(\sin(s^3p^3\,\Delta t)\,\hat{V}(p, t)))(X_j), \end{aligned} \tag{3.2}$$

which is likely to be more accurate than (3.1) in situations where dispersion dominates nonlinearity in (2.3). Indeed, the linear part of (3.2) is exactly satisfied by any solution of the linear part of (2.3). Furthermore, the linearised stability condition for (3.2) is

$$\Delta t < \left(\frac{2L}{N}\right)^3 0.1520, \tag{3.3}$$

whereas (3.1) is subject to the more restrictive condition $\Delta t < (2L/N)^3\,0.0323$. (See [5] for a linear stability analysis.)

Note that implementation of (3.2) requires three FFTs per time step.

(ii) *Semi-implicit scheme of Chan and Kerkhoven* [2]. Chan and Kerkhoven integrated the KdV equation in time in Fourier space, using a Crank–Nicolson method for the linear term and a leap-frog method for the nonlinear term. The nonlinear term, $6svv_X$, in (2.3) is initially re-written as w_X, where $w = 3sv^2$. In the algorithm below $W(X_j, t)$ denotes the approximation to $w(X_j, t)$.

ALGORITHM. Given $V(X_j, t)$, $V(X_j, t-\Delta t)$, $\hat{V}(p, t)$, $\hat{V}(p, t-\Delta t)$ for $j = 0, 1, \ldots, N-1$ and $p = -M, -M+1, \ldots, M-1$.

1. Form $W(X_j, t) = 3s[V(X_j, t)]^2$, $j = 0, 1, \ldots, N-1$.
2. Transform for $\hat{W}(p, t) = (F(W(\cdot, t)))(p)$, $p = -M, -M+1, \ldots, M-1$.
3. Solve

$$\begin{aligned} &\hat{V}(p, t+\Delta t) \\ &\quad = \hat{V}(p, t-\Delta t) - 2ip\,\Delta t\hat{W}(p, t) + i\Delta t s^3p^3[\hat{V}(p, t+\Delta t) + \hat{V}(p, t-\Delta t)] \end{aligned}$$

   for $\hat{V}(p, t+\Delta t)$, $p = -M, -M+1, \ldots, M-1$.

4. Invert for $V(X_j, t+\Delta t) = (F^{-1}(\hat{V}(\cdot, t+\Delta t)))(X_j)$, $j = 0, 1, \ldots, N-1$.

The semi-implicit method requires only two FFTs per time step. Apart from this favourable property a linear stability analysis indicates that the time step is not subject to the usual $O(N^{-3})$ restriction which appears in (3.3). The authors obtained linear stability conditions dependent on the relative magnitudes of the first and third derivative terms, and on the spectrum of frequencies being represented. For the 1- and 2-soliton test problems the linear stability restriction may be written as

$$(\Delta t)^2 < \frac{\sqrt{3}}{144\beta^3}, \tag{3.4}$$

where β denotes the maximum value of $|v|$ and is therefore $2k^2$ and $\frac{1}{2}\max(k_1^2, k_2^2)$ for the 1- and 2-soliton problems, respectively.

(iii) *Modified basis function scheme of Chan and Kerkhoven* [2]. This method uses solutions to the linear dispersive part of the KdV equation as basis functions for a pseudospectral method. The scheme is likely to be more accurate, therefore, in situations where dispersion dominates nonlinearity. An approximation to $v(X, t)$ is sought in the form

$$V(X, t) = \sum_{p=-M}^{M-1} \bar{V}(p, t)\, e^{i(pX + s^3p^3t)},$$

and $w = 3sv^2$ is replaced by an expansion of this type with coefficients $\bar{W}(p, t)$. Note that $\bar{V}(p, t) = \hat{V}(p, t)\, e^{-is^3p^3t}$ and $\bar{W}(p, t) = \hat{W}(p, t)\, e^{-is^3p^3t}$ in the notation used in (i) above. The method is conveniently represented in algorithmic form.

ALGORITHM. Given $\bar{V}(p, t)$, $\bar{V}(p, t-\Delta t)$ for $p = -M, -M+1, ..., M-1$.

1. Form $\hat{V}(p, t) = \bar{V}(p, t)\, e^{is^3p^3t}$, $p = -M, -M+1, ..., M-1$.
2. Invert for $V(X_j, t) = (F^{-1}(\hat{V}(\cdot, t)))(X_j)$, $j = 0, 1, ..., N-1$.
3. Form $W(X_j, t) = 3s[V(X_j, t)]^2$, $j = 0, 1, ..., N-1$.
4. Transform for $\hat{W}(p, t) = (F(W(\cdot, t)))(p)$
   and hence $\bar{W}(p, t) = \hat{W}(p, t)\, e^{-is^3p^3t}$, $p = -M, -M+1, ..., M-1$.
5. *Update* $\bar{V}$ *using*
   $\bar{V}(p, t+\Delta t) = \bar{V}(p, t-\Delta t) - 2ip\,\Delta t\, \bar{W}(p, t)$, $p = -M, -M+1, ..., M-1$.

As for the semi-implicit method, this algorithm requires only two FFTs per time step. A linear stability analysis gives the condition

$$\Delta t < \frac{L}{3N\pi\beta}, \tag{3.5}$$

where β is as defined in (3.4). This $O(N^{-1})$ condition is less restrictive than the Fornberg and Whitham condition (3.3).

3.2. *A New Split-Step Scheme Based on Taylor Expansion*

In this method we advance the solution of (2.3) in two stages at each time step: the first stage involves the solution of the nonlinear equation

$$v_t + 6svv_X = 0 \tag{3.6}$$

using a Lax–Wendroff [9] formulation of the Taylor expansion, and the output from this stage serves as an initial condition for the linear equation

$$v_t + s^3 v_{XXX} = 0. \tag{3.7}$$

To advance the solution of Eq. (3.6) we employ the identities

$$\frac{\partial^q v}{\partial t^q} = (-6s)^q \frac{\partial^q}{\partial X^q}\left(\frac{v^{q+1}}{q+1}\right), \qquad q = 1, 2, ...$$

satisfied by solutions of this equation. These enable us to write the Taylor expansion as

$$\begin{aligned} v(X, t+\Delta t) = v(X, t) &- (6s\,\Delta t)\frac{\partial}{\partial X}\left\{\frac{1}{2}\,[v(X, t)]^2\right\} \\ &+ \frac{1}{2}(6s\,\Delta t)^2 \frac{\partial^2}{\partial X^2}\left\{\frac{1}{3}\,[v(X, t)]^3\right\} \\ &- \frac{1}{6}(6s\,\Delta t)^3 \frac{\partial^3}{\partial X^3}\left\{\frac{1}{4}\,[v(X, t)]^4\right\} + O(\Delta t)^4. \end{aligned}$$

The discrete Fourier transform of $v(\cdot, t+\Delta t)$ is evaluated using terms up to $O(\Delta t)^3$ and this transform provides the initial condition for the solution of (3.7) in Fourier space. The split-step algorithm is presented below.

ALGORITHM. Given $V(X_j, t)$, $\hat{V}(p, t)$ for $j = 0, 1, ..., N-1$ and $p = -M, -M+1, ..., M-1$.

1. Form $W(X_j, t) = \frac{1}{2}[V(X_j, t)]^2$, $Y(X_j, t) = \frac{1}{3}V(X_j, t)\,W(X_j, t)$ and $Z(X_j, t) = \frac{1}{4}V(X_j, t)\,Y(X_j, t)$, $j = 0, 1, ..., N-1$.
2. Transform for $\hat{W}(p, t) = (F(W(\cdot, t)))(p)$, $\hat{Y}(p, t) = (F(Y(\cdot, t)))(p)$ and $\hat{Z}(p, t) = (F(Z(\cdot, t)))(p)$, $p = -M, -M+1, ..., M-1$.
3. For $p = -M, -M+1, ..., M-1$ set $\eta = 6sp\,\Delta t$ and form $\hat{V}^*(p, t+\Delta t) = \hat{V}(p, t) - i\eta\hat{W}(p, t) - \eta^2\hat{Y}(p, t) + i\eta^3\hat{Z}(p, t)$.
4. Form $\hat{V}(p, t+\Delta t) = \hat{V}^*(p, t+\Delta t)\,e^{ip^3s^3\Delta t}$, $p = -M, -M+1, ..., M-1$.
5. Invert for $V(X_j, t+\Delta t) = (F^{-1}(\hat{V}(\cdot, t+\Delta t)))(X_j)$, $j = 0, 1, ..., N-1$.

The expansion in step 3 must be taken as far as $O(\Delta t)^3$ to satisfy the linear stability condition and, as a result, four FFTs are required per time step.

Linear Stability

If the method is applied to the linear, constant coefficient equation

$$v_t + 6s\beta v_X + s^3 v_{XXX} = 0, \tag{3.8}$$

the solution in discrete Fourier space provided by the algorithm is

$$\hat{V}(p, t+\Delta t) = G(s, p, \beta, \Delta t)\, \hat{V}(p, t),$$

where $G(s, p, \beta, \Delta t) = [1 - i\beta\eta - \frac{1}{2}\beta^2\eta^2 + (i/6)\,\beta^3\eta^3]\, e^{ip^3s^3\,\Delta t}$.

Hence $|G|^2 = 1 + (\beta^4\eta^4/36)(\beta^2\eta^2 - 3)$ and the method is therefore linearly stable if $\beta^2\eta^2 < 3$ for $p = 0, 1, ..., M$.

The linear stability condition for the split-step scheme may therefore be written as

$$\Delta t < \frac{L}{\sqrt{3}\, N\pi\beta}. \tag{3.9}$$

It is readily shown that the numerical solution satisfies the discrete "mass" conservation condition $\sum_{k=0}^{N-1} V(X_k, t) = \text{constant}$. Combine steps 3 and 4 of the algorithm and note that

$$i\eta \hat{W}(p, t)\, e^{ip^3s^3\,\Delta t} = \frac{3s\,\Delta t i}{\sqrt{N}} \sum_{j=0}^{N-1} [V(X_j, t)]^2\, pz^{-jp} e^{ip^3s^3\,\Delta t} = \rho(p),$$

say, where z is an Nth root of unity and is given by $z = e^{2\pi i/N}$. Hence

$$(F^{-1}(\rho(\cdot)))(X_k) = \frac{3s\,\Delta t i}{N} \sum_{j=0}^{N-1} \sum_{p=-M}^{M-1} [V(X_j, t)]^2\, pz^{(k-j)p} e^{ip^3s^3\,\Delta t}$$

and the summation $\sum_{k=0}^{N-1} (F^{-1}(\rho(\cdot)))(X_k)$ is trivially zero.

The contribution to the total mass arising from the term involving $\hat{W}$ in step three is therefore zero, and analogous results hold for the terms involving $\hat{Y}$ and $\hat{Z}$. The contribution from the term involving $\hat{V}$ is

$$\sum_{j=0}^{N-1} \sum_{p=-M}^{M-1} V(X_j, t)\, z^{-jp} e^{ip^3s^3\,\Delta t}\, \delta_{o,p},$$

where $\delta_{o,p}$ is the Kronecker delta. The conservation result now follows immediately.

Split-Step Error

A question which one might ask in relation to the split-step scheme described in this section is whether or not time splitting introduces significant discretisation errors. This question has been addressed, inter alios, by Strang [16] and by Leveque and Oliger [10]. A recent paper by Sanz-Serna and Verwer [13] also considered this matter in the context of time-splitting for nonlinear dispersive wave equations.

To examine split-step errors for the spectral method considered here we are at liberty to ignore spatial discretisation errors and consider only errors associated with the time discretisation. For convenience, drop the X dependence and let $v^*(t+\Delta t)$ be the solution of the nonlinear equation (3.6) given by the expansion method. The final solution at time $t+\Delta t$ given by the two-stage process may be written as

$$v(t+\Delta t)=[1-s^3\,\Delta t\,D^3+\tfrac{1}{2}s^6\,\Delta t^2\,D^6-\tfrac{1}{6}s^9\,\Delta t^3\,D^9+\cdots]\,v^*(t+\Delta t), \quad (3.10)$$

where $D\equiv\partial/\partial t$. The linear stage of the solution is exact and the above expansion may therefore be regarded as infinite in extent. If the solution of the complete equation (2.3) given by an analogous method is denoted by $v^{(c)}(t+\Delta t)$ then the split-step error is

$$E_{\text{split}}=v^{(c)}(t+\Delta t)-v(t+\Delta t)=-9s^4\,\Delta t^2[D(v)\,D^3(v)+(D^2(v))^2]+O(\Delta t)^3,$$

where $v\equiv v(t)$. This error arises from the non-commutativity of the linear and nonlinear spatial differentiation operators and one notes, for example, that if the method is applied to the linear, constant coefficient equation (3.8) then $E_{\text{split}}=0$.

The total error involved in integrating from time t to time $t+\Delta t$ is the sum of E_{split} and the discretization error of the nonlinear step. Since the expansion used contains terms up to $O(\Delta t)^3$ it follows that the total error is dominated by E_{split}. Strang [16] has shown that E_{split} may be improved if the operators are applied in a symmetric manner. If we denote the solution (3.10) by

$$v(t+\Delta t)=\mathscr{L}(\Delta t)\,v^*(t+\Delta t)=\mathscr{L}(\Delta t)\,\mathscr{N}(\Delta t)\,v(t),$$

where $\mathscr{L}$ and $\mathscr{N}$ are the linear and nonlinear operators, respectively, then the symmetric implementation has the form

$$v(t+\Delta t)=\mathscr{N}\left(\frac{\Delta t}{2}\right)\mathscr{L}(\Delta t)\,\mathscr{N}\left(\frac{\Delta t}{2}\right)v(t). \quad (3.11)$$

It is readily shown that for this method $E_{\text{split}}=O(\Delta t)^3$ and the complete solution process is then second order in time. If integration is performed over a large number of steps between printouts the half-step operations in (3.11) are only required at the beginning and at the end of the sequence of steps. Henceforth, we assume that any split-step calculations referred to in this paper are performed using the symmetric implementation (3.11).

3.3. *A New Split-Step Scheme Based on Characteristics*

Here again we split the operator and solve (3.6) followed by (3.7) to advance the solution over one time step. Since the solution $v(X, t)$ of (3.6) is constant along any integral curve of the characteristics equation $dX/dt=6sv$ we can deduce that

$$v(X_j, t+\Delta t)=v(\xi_j, t), \quad (3.12)$$

where $X_j = \xi_j + 6s\,\Delta t\, v(\xi_j, t)$. If we write $\xi_j = X_j + \theta_j\,\Delta X$ then θ_j is the solution of

$$\theta_j + 6s\lambda v(X_j + \theta_j\,\Delta X, t) = 0, \tag{3.13}$$

where $\lambda = \Delta t/\Delta X$. This equation is solved approximately using a fixed-point iteration in which $v(X_j + \theta_j\,\Delta X, t)$ is replaced by a polynomial interpolant $P_j^{(2l)}$ $(\theta_j; \Delta X, t)$ of degree $2l$ which fits the computed solution $V(\cdot, t)$ at $2l+1$ nodes in the neighbourhood of X_j. The approximation to θ_j is given by the iteration

$$\begin{aligned} \theta_j^{(1)} &= -6s\lambda V(X_j, t), \\ \theta_j^{(\nu+1)} &= -6s\lambda P^{(2l)}(\theta_j^{(\nu)}; \Delta X, t), \qquad \nu = 1, 2, ... \end{aligned} \tag{3.14}$$

and the solution of the nonlinear step is then given by (3.12) in the form

$$V^*(X_j, t+\Delta t) = P_j^{(2l)}(\theta_j; \Delta X, t). \tag{3.15}$$

For the 1- and 2-soliton problems $V^*(X_j, t+\Delta t)$ is the set to zero at nodes near the boundaries then (3.14) and (3.15) are used at the remaining nodes. The integration from t to $t+\Delta t$ is described below.

ALGORITHM. Given $V(X_j, t)$ for $j = 0, 1, ..., N$.

1: $V^*(X_j, t+\Delta t) := 0$ for $j = 0, 1, ..., l-1$ and $j = N-l+1, N-l+2, ..., N$.

2: $V^*(X_j, t+\Delta t)$ given by (3.14) and (3.15) for $j = l, l+1, ..., N-l$.

3: Transform for $\hat{V}^*(p, t-\Delta t) = (F(V^*(\cdot, t+\Delta t)))(p)$, $p = -M, -M+1, ..., M-1$.

4: Continue with steps 4 and 5 of the algorithm in Section 3.2 and complete the cycle with $V(X_N, t+\Delta t) := 0$.

The characteristics pseudospectral method requires only two FFTs per time step and the operations are performed symmetrically, as in (3.11).

Linear Stability

If the method is applied to the linear equation (3.8) the intermediate solution is

$$V^*(X_j, t+\Delta t) = P_j^{(2l)}(\theta; \Delta X, t),$$

where $\theta = -6s\lambda\beta$. To simplify the analysis let $l = 1$ and obtain

$$V^*(X_j, t+\Delta t) = \tfrac{1}{2}\,[\theta(\theta-1)\,V(X_{j-1}, t) + 2(1-\theta^2)\,V(X_j, t) + \theta(\theta+1)\,V(X_{j+1}, t)].$$

This equation may be transformed to Fourier space by means of (2.4) to give

$$\hat{V}^*(p, t+\Delta t) = \tfrac{1}{2}\,[\theta(\theta-1)\,e^{-i\eta_p} + 2(1-\theta^2) + \theta(\theta+1)\,e^{i\eta_p}]\,\hat{V}(p, t),$$

where $\eta_p = 2\pi p/N$. Hence

$$\hat{V}(p, t+\Delta t) = G(s, p, \theta, \Delta t)\,\hat{V}(p, t),$$

where

$$G(s, p, \theta, \Delta t) = [\theta^2 \cos \eta_p + \theta i \sin \eta_p + 1 - \theta^2]\, e^{ip^3 s^3 \Delta t}.$$

Hence $|G|^2 = 1 + \theta^2(\cos \eta_p - 1)^2\, (\theta^2 - 1)$ and the method is therefore linearly stable if $|\theta| < 1$, or,

$$\Delta t < L/3N\beta. \tag{3.16}$$

Similar $O(N^{-1})$ restrictions may be derived for higher values of l: for example, if $l = 2$ the linear stability condition is $|\theta| < 2$. The results in Section 4 were obtained using the value $l = 3$.

3.4. *A Quasi-Newton Implicit Scheme*

For notational convenience we denote the discrete approximations to v, v_X, and v_{XXX} at $(X_j, n\,\Delta t)$ by V_j^n, $(V_X)_j^n$, and $(V_{XXX})_j^n$, respectively, and we write the fully implicit pseudospectral scheme as

$$\begin{aligned} V_j^{n+1} - V_j^n + \tfrac{3}{2} s\, \Delta t \{ [V_j^{n+1} + V_j^n][(V_X)_j^{n+1} + (V_X)_j^n] \} \\ + \tfrac{1}{2} s^3\, \Delta t [(V_{XXX})_j^{n+1} + (V_{XXX})_j^n] = 0. \end{aligned} \tag{3.17}$$

This provides a system of N nonlinear equations for $V(\cdot, (n+1)\,\Delta t)$ which may be written for $j = 1, 2, ..., N$ as

$$\mathscr{R}_j = \mathscr{F}_j(V(\cdot, (n+1)\,\Delta t), V(\cdot, n\,\Delta t)) + \mathscr{H}_j(V(\cdot, n\,\Delta t)) = 0, \tag{3.18}$$

where

$$\begin{aligned} \mathscr{F}_j = V_j^{n+1} + \tfrac{3}{2} s\, \Delta t \{ (V_X)_j^{n+1}\, (V_j^{n+1} + V_j^n) + V_j^{n+1} (V_X)_j^n \} \\ + \tfrac{1}{2} s^3\, \Delta t (V_{XXX})_j^{n+1} \end{aligned} \tag{3.19}$$

and

$$\mathscr{H}_j = -V_j^n + \tfrac{3}{2} s\, \Delta t\, V_j^n (V_X)_j^n + \tfrac{1}{2} s^3\, \Delta t (V_{XXX})_j^n. \tag{3.20}$$

To solve (3.18) by a Newton iteration we require the Jacobian $\partial \mathscr{F}_j / \partial V_l^{n+1}$ ($j, l = 1, 2, ..., N$), and this is a complicated operation if the derivatives are evaluated by Fourier transformation. Here we propose to use a quasi-Newton method in which the derivatives $(V_X)_j^{n+1}$ and $(V_{XXX})_j^{n+1}$ in $\mathscr{F}_j$ are approximated by second-order central differences during the formation of the Jacobian. Accordingly, $(V_X)_j^{n+1}$ and $(V_{XXX})_j^{n+1}$ are replaced by the assignments

$$(V_X)_j^{n+1} := \frac{1}{2\Delta X} (V_{j+1}^{n+1} - V_{j-1}^{n+1}) \tag{3.21}$$

of6 Tw 48t 1738472V7r Vi"+:s3i81 =8lc 2 7:7Tr and

$$(V_{XXX})_j^{n+1} := \frac{1}{2(\Delta X)^3}\left[V_{j+2}^{n+1} - 2(V_{j+1}^{n+1} - V_{j-1}^{n+1}) - V_{j-2}^{n+1}\right]. \tag{3.22}$$

With these approximations the Jacobian has a pentadiagonal structure, and if $\mathscr{F}_{j,l}$ denotes $\partial\mathscr{F}_j/\partial V_l^{n+1}$ then

$$\begin{aligned} \mathscr{F}_{j,j+2} = -\mathscr{F}_{j,j-2} = \kappa, \qquad \mathscr{F}_{j,j+1} = -\mathscr{F}_{j,j-1} = -2\kappa + \rho(V_j^{n+1} + V_j^n), \\ \mathscr{F}_{j,j} = 1 + \rho(V_{j+1}^{n+1} - V_{j-1}^{n+1}) + 2\Delta X\rho(V_X)_j^n, \end{aligned} \tag{3.23}$$

where

$$\kappa = \frac{s^3\,\Delta t}{4(\Delta X)^3} \quad \text{and} \quad \rho = \frac{3s\,\Delta t}{4\Delta X}.$$

The elements in the top right-hand corner and in the bottom left-hand corner of the Jacobian are set to zero. The 1- and 2-soliton solutions vanish near the boundaries so the corner contributions may be ignored. In the algorithm below the approximations to $V(\cdot, (n+1)\,\Delta t)$ are denoted by $W^{(\nu)}$, $\nu = 0, 1, ...,$ and the jth component of $W^{(\nu)}$ is $W_j^{(\nu)}$.

ALGORITHM. Given V_j^n, $(V_X)_j^n$, and $(V_{XXX})_j^n$ for $j = 1, 2, ..., N$.

```
1. Form $\mathscr{H}_j(V(\cdot, n\,\Delta t))$ using (3.20).
2. $W_j^{(0)} := V_j^n - 6s\,\Delta t\, V_j^n(V_X)_j^n - s^3\,\Delta t(V_{XXX})_j^n,\ j = 1, 2, ..., N.$
3. Form the Jacobian, $\mathscr{J}$, as in (3.23) using $W_j^{(0)}$, $V_j^n$, and $(V_X)_j^n, j = 1, 2, ..., N$.
   Factorise $\mathscr{J}$.
4. $\nu := 0$.
5. $\mathscr{R}_j := \mathscr{F}_j(W^{(\nu)}, V(\cdot, n\Delta t)) + \mathscr{H}_j(V(\cdot, n\Delta t)),\ j = 1, 2, ..., N.$
6. Solve $\mathscr{J}E = -\mathscr{R}$, where $\mathscr{R} = [\mathscr{R}_1, \mathscr{R}_2, ..., \mathscr{R}_N]^T$, then
   $W^{(\nu+1)} := W^{(\nu)} + E$ and $\nu := \nu + 1$.
7. If $\nu < \max \nu$ go to 5.
8. $V_j^{n+1} := W_j^{(\nu)},\ (V_X)_j^{n+1} := (W_X^{(\nu-1)})_j,\ (V_{XXX})_j^{n+1} := (W_{XXX}^{(\nu-1)})_j,\ j = 1, 2, ..., N.$
```

With $\max \nu = 1$ the algorithm requires three FFTs per time step. Accuracy could be improved by evaluating derivatives in terms of $W^{(\nu)}$ at step 8, or by increasing $\max \nu$.

4. NUMERICAL RESULTS

4.1. *Soliton Test Problems*

The 1- and 2-soliton problems described in Section 2 were solved numerically on a discretisation of $(x, t) \in [-L, L] \times [0, T]$ using the six pseudospectral methods which were discussed in Section 3. For each test integration we fixed the maximum acceptable point-wise error—denoted by L_∞—and adjusted parameters to minimise CPU time. Tables I–IV show the computed results for 1- and 2-solitons on the interval $[-20, 20]$. Initial conditions were given by (2.1) and (2.2), with k, k_1, and k_2 chosen to give the specified amplitudes. The tables show grid spacings $\Delta x = 2L/N$ and Δt, CPU s, the L_∞ error at the terminating time T, and relative errors EC1 and EC2 in discrete approximations to the integrals (2.6) and (2.7). Computations were performed on a VAX 8650 computer.

The computed results show that the semi-implicit scheme of Chan and Kerkhoven [2] is the most efficient of the methods tested. The split-step expansion scheme is the second most efficient method and it almost becomes competitive with the best scheme for the 2-soliton test. The split-step scheme involves only two time levels and this is an advantage in extensions to more than one space dimension. The Fornberg–Whitham scheme is comparable with the second Chan–Kerkhoven scheme and their computational efficiency is approximately half that of the best scheme. The characteristics scheme performs as well as the Fornberg–Whitham scheme for the 1-soliton problem but it encounters difficulties in the second test: indeed, it failed to reach the prescribed accuracy in the large-amplitude 2-soliton case. The results produced by the implicit quasi-Newton scheme are interesting: this method improves in efficiency relative to the others as the numerical difficulties increase. The method was effected crudely with max $\nu = 1$ and the results suggest that a more careful implementation might produce a good method for situations where accuracy rather than computational efficiency is important. This method requires further investigation.

TABLE I

Comparison of Computing Times for 1 Soliton with Amplitude 1 and Initial Location $x = 0$ on $(x, t) \in [-20, 20] \times [0, 1]$

Scheme	Δx Δt	CPU s	L_∞	EC1	EC2
(i) Fornberg and Whitham	0.625 0.0186	0.74	0.0049	0.0039	0.024
(ii) Chan and Kerkhoven I	0.625 0.0318	0.17	0.0049	0.0022	0.020
(iii) Chan and Kerkhoven II	0.625 0.0141	0.55	0.0048	0.0035	0.028
(iv) Split-step expansion	0.625 0.0333	0.32	0.0046	0.0044	0.022
(v) Split-step characteristics	0.3125 0.0458	0.58	0.0049	0.000080	0.033
(vi) Quasi-Newton	0.625 0.0453	1.40	0.0050	0.0026	0.024

Note. L_∞ is the point-wise error at $t = 1$ and EC1 and EC2 give relative errors in approximations to the conservation integrals (2.6) and (2.7). Accuracy constraint imposed is $L_\infty \leqslant 0.005$.

TABLE II

Comparison of Computing Times for 1 Soliton with Amplitude 2 and Initial Location $x=0$ on $(x, t) \in [-20, 20] \times [0, 2]$

	Scheme	Δx Δt	CPU s	L_∞	EC1	EC2
(i)	Fornberg and Whitham	0.3125 0.0045	7.38	0.0075	0.00066	0.0047
(ii)	Chan and Kerkhoven I	0.3125 0.006	3.74	0.0079	0.000020	0.00056
(iii)	Chan and Kerkhoven II	0.3125 0.0031	9.56	0.0075	0.00013	0.0018
(iv)	Split-step expansion	0.3125 0.007	5.70	0.0076	0.00029	0.0018
(v)	Split-step characteristics	0.1562 0.0117	7.81	0.0081	0.00042	0.0042
(vi)	Quasi-Newton	0.625 0.012	4.28	0.0076	0.0021	0.0034

Note. L_∞ is the point-wise error at $t=2$ and EC1 and EC2 give relative errors in approximations to the conservation integrals (2.6) and (2.7). Accuracy constraint imposed is $L_\infty \leqslant 0.008$.

TABLE III

Comparison of Computing Times for 2 Solitions with Amplitudes 0.5 and 1 and Initial Locations $x=0$ and $x=-2$, Respectively, on $(x, t) \in [-20, 20] \times [0, 2]$

	Scheme	Δx Δt	CPU s	L_∞	EC1	EC2
(i)	Fornberg and Whitham	0.625 0.0185	0.95	0.0020	0.0012	0.0087
(ii)	Chan and Kerkhoven I	0.625 0.024	0.45	0.0019	0.0012	0.0091
(iii)	Chan and Kerkhoven II	0.625 0.0133	1.24	0.0020	0.0016	0.0064
(iv)	Split-step expansion	0.625 0.0431	0.50	0.0016	0.00076	0.0088
(v)	Split-step characteristics	0.3125 0.0032	9.25	0.0021	0.00055	0.0040
(vi)	Quasi-Newton	0.625 0.0022	2.33	0.0019	0.00024	0.0010

Note. L_∞ is the point-wise error at $t=2$ and EC1 and EC2 give relative errors in approximations to the conservation integrals (2.6) and (2.7). Accuracy constraint imposed is $L_\infty \leqslant 0.002$.

TABLE IV

Comparison of Computing Times for 2 Solitons with Amplitudes 0.5 and 2.5 and Initial Locations $x=0$ and $x=-4.8$, respectively, on $(x, t) \in [-20, 20] \times [0, 4]$

Scheme	Δx Δt	CPU s	L_∞	EC1	EC2
(i) Fornberg and Whitham	0.3125 0.0029	24.88	0.015	0.000037	0.0023
(ii) Chan and Kerkhoven I	0.3125 0.0042	10.57	0.019	0.00019	0.0027
(iii) Chan and Kerkhoven II	0.3125 0.0020	25.60	0.015	0.00025	0.010
(iv) Split-step expansion	0.3125 0.0052	16.28	0.019	0.00015	0.0034
(v) Split-step characteristics	0.1562 0.0035	*	*	*	*
(vi) Quasi-Newton	0.625 0.0050	19.95	0.020	0.0021	0.022

Note. L_∞ is the point-wise error at $t=4$ and EC1 and EC2 give relative errors in approximations to the conservation integrals (2.6) and (2.7). Accuracy constraint imposed is $L_\infty \leqslant 0.02$.

As states in Section 1, difference schemes should ideally simulate the conservation conditions of the differential equations which are being approximated. It is a simple matter to modify some of the above schemes so that, at least for the discretisation in space, energy conservation is achieved. Such modifications are advisable in situations where accuracy rather than computational efficiency is of prime importance. We shall see that the semi-discrete conservation condition is obtained at an additional computational cost.

Suppose the semi-discrete equations are written as a system of nonlinear ordinary differential equations in the form

$$d\mathbf{V}/dt = \mathbf{F}(\mathbf{V}), \tag{4.1}$$

where $\mathbf{V} = \mathbf{V}(t) = [V(X_0, t), V(X_1, t), ..., V(X_{N-1}, t)]^T$. If the discretisation is such that $\mathbf{V}^T\mathbf{F} = 0$ then $(d/dt)(\mathbf{V}^T\mathbf{V}) = 0$ and energy is conserved. This conservation condition can be extended to the fully-discrete system if discretisation in time is effected by means of the scheme

$$\mathbf{V}^{n+1} - \mathbf{V}^n = \Delta t\, \mathbf{F}(\tfrac{1}{2}(\mathbf{V}^n + \mathbf{V}^{n+1})) \tag{4.2}$$

in the obvious notation. These conditions have been discussed by Sanz-Serna [12].

Consider, for example, the semi-discrete system derived from the Fornberg–Whitham scheme (3.1) by forming the limit as $\Delta t \to 0$. This limiting process yields the ordinary differential equation

$$\dot{V}(X_j, t) = F_j = -6sV(X_j, t)\, V'(X_j, t) + s^3 V'''(X_j, t), \tag{4.3}$$

where the dot denotes differentiation with respect to time and the spatial derivatives are

$$V'(X_j, t) = \frac{i}{N} \sum_{p=-M}^{M-1} \sum_{k=0}^{N-1} p z^{p(j-k)} V(X_k, t)$$

and

$$V'''(X_j, t) = -\frac{i}{N} \sum_{p=-M}^{M-1} \sum_{k=0}^{N-1} p^3 z^{p(j-k)} V(X_k, t),$$

with $z = \exp(2\pi i/N)$. It is readily shown that $\sum_{j=0}^{N-1} V(X_j, t)\, F_j \neq 0$ and the condition $\mathbf{V}^T\mathbf{F} = 0$ is therefore not satisfied. However, if the first term on the right-hand side of (4.3) is modified to

$$-\frac{2si}{N} \sum_{p=-M}^{M-1} \sum_{k=0}^{N-1} p z^{p(j-k)} V(X_k, t)[V(X_k, t) + V(X_j, t)]$$

then energy conservation is achieved. The modification involves the approximation of vv_X at (X_j, t) by

$$\tfrac{1}{3}V(X_j, t)(F^{-1}(ip\hat{V}(p, t)))(X_j) + \tfrac{1}{3}(F^{-1}(ip\hat{W}(p, t)))(X_j),$$

where

$$\hat{W}(p, t) = (FW(\cdot, t))(p) \qquad \text{and} \qquad W(X_j, t) = [V(X_j, t)]^2.$$

It is immediately obvious that if leap-frog time discretisation is employed the [redacted]

To illustrate the beneficial effect of semi-discrete energy conservation we integrated the 2-soliton problem on a discretisation of $(x, t) \in [-20, 20] \times [0, T]$. In this test we fixed Δt and Δx and measured the L_∞ error and the conservation errors EC1 and EC2 at the terminating time T. Table V compares results given by

TABLE V

Comparison of Scheme (3.1) with Semi-Discrete Energy Conserving Modification

Scheme	Δx Δt	CPU s	L_∞	EC1	EC2
Leap-frog (3.1)	0.3125 0.0023	32.01	0.0091	0.00063	0.0079
Modified (3.1)	0.3125 0.0023	50.02	0.0052	0.000050	0.0079

Note. Results are for 2 solitons with amplitudes 0.5 and 2.5 and initial locations $x = 0$ and $x = -5$, respectively, on $(x, t) \in [-20, 20] \times [0, 4]$. L_∞ is the point-wise error at $t = 4$ and EC1 and EC2 give relative errors in approximations to conservation integrals (2.6) and (2.7).

scheme (3.1) with those given by the leap-frog discretisation of the semi-discrete energy conserving scheme described above.

It can be seen that the modified scheme is more accurate and, as might be expected, it gives a better approximation to the first invariant of the KdV equation. Note, of course, that the modified scheme required more computing time for a fixed number of time steps.

The energy conservation achieved by modifying (3.1) is destroyed by the explicit time discretisation. The fully discrete energy conservation condition $[\mathbf{V}(t_n)]^T \mathbf{V}(t_n) = \text{constant}$ is obtained by implicit time discretisation as on (4.2). This is best illustrated for the quasi-Newton implicit scheme (vi). To achieve energy conservation, (3.17) is modified to

$$V_j^{n+1} - V_j^n + \frac{s\,\Delta t}{2}\{[V_j^{n+1} + V_j^n][(V_X)_j^{n+1} + (V_X)_j^n] + (V_j^n + V_j^{n+1})_X^2\}$$

$$+ \tfrac{1}{2}s^3\,\Delta t[(V_{XXX})_j^{n+1} + (V_{XXX})_j^n] = 0, \tag{4.4}$$

where $(V_j^n + V_j^{n+1})_X^2 = (F^{-1}(ip\hat{W}(p, t_{n+\frac{1}{2}})))(X_j)$, with

$$\hat{W}(p, t_{n+\frac{1}{2}}) = (F(W(\cdot, t_{n+\frac{1}{2}})))(p)$$

and

$$W(X_j, t_{n+\frac{1}{2}}) = [V(X_j, n\,\Delta t) + V(X_j, (n+1)\,\Delta t)]^2.$$

This modification leads to a related change in the Jacobian elements (3.23).

4.2. *Recurrence Tests*

A demanding test of the accuracy of a method over a long integration period is provided by the ability of the method to reproduce the recurrence phenomenon first described by Zabusky and Kruskal [20]. The reader is referred to the original paper for details. Here it will suffice to say that a KdV equation is integrated on $0 \leqslant x \leqslant 2$, $t \geqslant 0$ using the initial condition $\cos \pi x$ and periodic boundary conditions. As time evolves the wave steepens and eventually breaks up to form eight solitons. These recombine in stages and the initial state is reproduced at $t = T_R$, where T_R is approximately 9.7 for the parameters which are employed. In principle, this recombination, or recurrence, should occur at times which are integer multiples of T_R. Here we examine the ability of some of the pseudospectral methods of Section 3 to reproduce the first recombination of solitons at $t = T_R$.

We found that the best results on the recurrence problem were produced by the semi-implicit scheme of Chan and Kerkhoven. Figure 1 shows the solution produced by thiş scheme at several values of time up to $t = T_R$. Apart from this semi-implicit method the only scheme which performed well on the recurrence problem was the split-step expansion method. This method reproduced the two solitons at $t = \frac{1}{2}T_R$, but the solution at $t = T_R$ is a poor imitation of the initial profile: this is seen in Fig. 2. The solutions produced by the other four methods

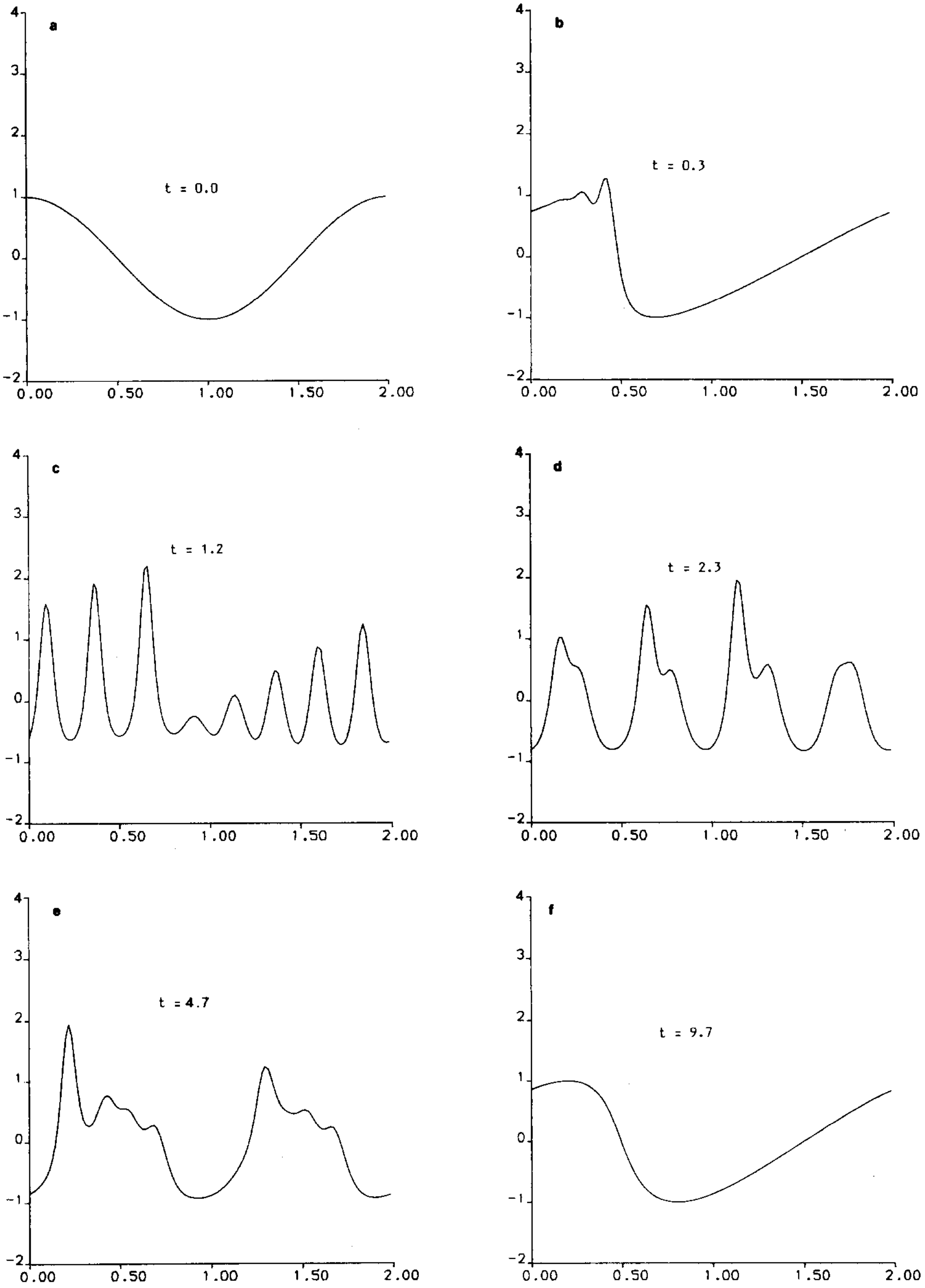

FIG. 1. Solution of the recurrence problem by Chan–Kerkhoven I. The figures show the solution profile at the specified times. Results were obtained using $N = 128$ and $\Delta t = 0.0035$.

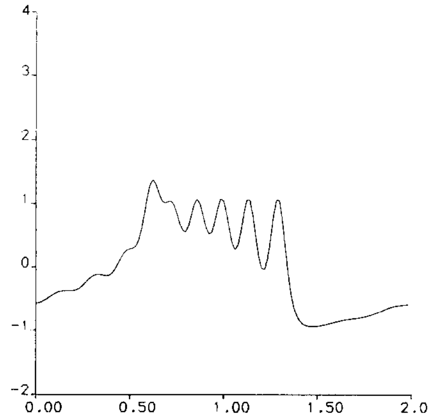

FIG. 2. Solution of the recurrence problem at $t = 9.7$ by the split-step expansion method. Results were obtained using $N = 256$ and $\Delta t = 1.14 \times 10^{-4}$.

became unstable before $t = 6$, whereas the semi-implicit and the split-step expansion schemes were integrated to $t = 2T_R$ with no evidence of blowup. It is of interest to note that the Fornberg–Whitham scheme became unstable at approximately $t = 5.6$, while the semi-conservative modification of this scheme did not exhibit blowup until $t = 15$. This demonstrates the stabilising effect of the conservation property.

5. CONCLUSIONS

Six Fourier pseudospectral methods have been tested for computational efficiency and accuracy. The best scheme in all the tests is the scheme by Chan and Kerkhoven [2] which integrates in Fourier space using 2 FFTs per time step. The scheme treats the nonlinear term using leap-frog in time and it therefore uses three time levels. A useful scheme which uses only two time levels is the split-step expansion scheme. The one-step property should be useful in extensions to two spaces dimensions.

It has been shown that many schemes can be made conservative with respect to the space discretisation at an increased computational cost. The advantages to be gained by this conservation property have been demonstrated. A fully discrete, implicit scheme which is energy-conserving has been discussed. This scheme requires further investigation.

It is of some interest to know how the best Fourier pseudospectral method identified in this study compares with the best method in the study by Taha and Ablowitz [17]. Accordingly, the Chan and Kerkhoven scheme was compared with the Taha and Ablowitz local scheme on the 1- and 2-soliton problems. The reader is referred to the paper by Taha and Ablowitz [17] for details of their local scheme. Table VI shows the normalised computing times for tests 1, 2, 3, and 4, where test

TABLE VI

	Test 1	Test 2	Test 3	Test 4
Chan and Kerkhoven I				
Δx	0.625	0.4	0.625	0.4
Δt	0.032	0.0058	0.024	0.0042
L_∞	0.0049	0.0075	0.0020	0.019
Normalised CPU	1	1	1	1
Taha and Ablowitz local				
Δx	0.2857	0.1333	0.1538	0.07143
Δt	0.21	0.05	0.16	0.05
L_∞	0.0047	0.0053	0.0018	0.013
Normalised CPU	0.76	0.88	1.40	1.43

i is that described by table i ($i = 1, 2, 3, 4$). The computing times are normalised so that the Chan and Kerkhoven time is one unit for each of the tests.

In the comparison of pseudospectral methods as described in Tables I–IV the selection of data parameters was simplified by constraining N to be a power of 2. The FFT algorithm used is efficient provided N contains no factors other than powers of the primes 2, 3, and 5, and this flexibility has been exploited in Table VI.

The results show that the local scheme is more efficient than the pseudospectral scheme on the 1-soliton problem, but less efficient on the more difficult 2-soliton problem. However, the differences in computing times are not large, and the results support the claim by Taha and Ablowitz that finite difference schemes based on the inverse scattering transform (IST) provide good approximations for equations which are solvable by the IST.

Acknowledgment

One of us (FZN) acknowledges the receipt of a Research Studentship from the Ministry of Higher Studies, Algeria.

References

1. M. E. Alexander and J. Ll. Morris, *J. Comput. Phys.* **30**, 428 (1979).
2. T. F. Chan and T. Kerkhoven, *SIAM J. Numer. Anal.* **22**, 441 (1985).
3. R. K. Dodd, J. C. Eilbeck, J. D. Gibbon, and H. C. Morris, *Solitons and Nonlinear Wave Equations* (Academic Press, New York, 1982).
4. B. Fornberg, *Geophysics* **52**, 483 (1987).
5. B. Fornberg and G. B. Whitham, *Philos. Trans. Roy. Soc. London* **289**, 373 (1978).
6. C. S. Gardner, J. M. Greene, M. D. Kruskal, and R. M. Miura, *Commun. Pure Appl. Math.* **27**, 97 (1974).

7. R. Hirota, *Phys. Rev. Lett.* **27**, 1192 (1971).
8. D. J. Korteweg and G. de Vries, *Philos. Mag.* **39**, 422 (1895).
9. P. D. Lax and B. Wendroff, *Commun. Pure Appl. Math.* **17**, 381 (1964).
10. R. J. Leveque and J. Oliger, *Math. Comput.* **40**, 469 (1983).
11. J. M. Sanz-Serna and I. Christie, *J. Comput. Phys.* **39**, 94 (1981).
12. J. M. Sanz-Serna, *J. Comput. Phys.* **47**, 199 (1982).
13. J. M. Sanz-Serna and J. G. Verwer, *IMA J. Numer. Anal.* **6**, 25 (1986).
14. H. Schamel and K. Elsasser, *J. Comput. Phys.* **22**, 501 (1976).
15. S. W. Schoombie, *IMA J. Numer. Anal.* **2**, 95 (1982).
16. G. Strang, *SIAM J. Numer. Anal.* **5**, 506 (1968).
17. T. R. Taha and M. J. Ablowitz, *J. Comput. Phys.* **55**, 231 (1984).
18. F. Tappert, *Lect. Appl. Math. Amer. Math. Soc.* **15**, 215 (1974).
19. A. C. Vliegenthart, *J. Eng. Math.* **5**, 137 (1971).
20. N. J. Zabusky and M. D. Kruskal, *Phys. Rev. Lett.* **15**, 240 (1965).